Precision Injury Mapping in Tendon: Isolating Cell Necrosis and ECM Micro-Ruptures with Amplified Femtosecond Laser Ablation

Diane Stonestreet[1], Robert F. Hawkins[1], Nozomi Nishimura[1], Nelly Andarawis-Puri[1,2]
[1]Cornell University, Ithaca, NY, [2]Hospital for Special Surgery, New York, NY
ds978@cornell.edu

Disclosures: Diane Stonestreet (N), Robert F. Hawkins (N), Nozomi Nishimura (N), Nelly Andarawis-Puri (N)

INTRODUCTION: Tendon injuries are a major clinical burden,[1] with overuse tendinopathies marked by excessive cell death, abnormal inflammatory signaling, and disrupted extracellular matrix architecture (ECM).[2] While some inflammatory cells are present in these injuries, the response is insufficient and ineffective,[3] as highlighted by the limited efficacy of anti-inflammatory treatments such as NSAIDs.[4] Ultimately, sub-rupture damage, the hallmark of early tendinopathy, progressively weakens the ECM, predisposing tendons to acute rupture.. Clinical interventions like dry needling attempt to break this cycle by inducing localized cell necrosis and micro-ruptures, yet their outcomes are inconsistent[5] likely due to variable effects on ECM, cells, and vasculature, each driving different and potentially confounding biological responses. We aim to test the hypothesis that each tendon structural component—ECM, and cells—generates distinct immune-activating signals upon injury, with ECM damage inducing catabolic, non-inflammatory signaling, cell necrosis triggering canonical pro-inflammatory cascades that recruit macrophages, and not all of these signals contributing to effective healing. To dissect these component-specific responses, we optimized amplified femtosecond laser (AFL) ablation *in vivo* to selectively induce cell and ECM damage.[6]

METHODS: All studies were approved by IACUC. *Cell Ablation:* C57BL/6 (B6) and Cx3Cr1^{GFP}-CCR2^{RFP} mice (n =17, both sexes) were used to optimize cell ablation. Animals were injected with Hoechst 33342 to label cell nuclei and injected with propidium iodide (PI) to stain dead cells. *In vivo* Second Harmonic Generation (SHG) imaging and two-photon fluorescence guided AFL ablation was used to induce cell necrosis. Laser pulse energies ranged from 20–500nJ with 1–20 pulses. Z-stack images were collected immediately before, 5 minutes after, and 10 minutes after ablation. *ECM Ablation:* B6 and Cx3Cr1^{GFP}-CCR2^{RFP} mice (n = 8, both sexes) were used to optimize ECM ablation and were subject to the same injections and *in vivo* imaging described above. To induce ECM damage, ablation was performed at varying tissue depths (5-60µm) with a range of ablation pulse energies (250-1300nJ) and pulse counts (1-3000). Z-stack images were taken immediately before and after ablation to assess loss of SHG signal and cell death. *Statistics:* Statistical analysis has only been performed on the cell ablation data thus far. Hoechst area, Hoechst mean intensity, and PI mean intensity were evaluated using a Friedman Test with Dunn's Multiple Comparisons ($p < 0.05$), while PI stain area was assessed using a Wilcoxon Matched-Pairs Signed Rank Test ($p < 0.05$).

RESULTS: *Cell Ablation:* Hoechst staining enabled precise identification of tenocyte nuclei to depths of 50–80 µm. Ablation energies of ~40nJ with 20 pulses resulted in an immediate increase in PI signal (Fig. 1B) which spread throughout the cell nucleus and increased in intensity in the minutes following the ablation (Fig. 1C, 1F, 1G), indicative of early necrotic changes, without disruption of ECM SHG signal. Hoechst fluorescence remained stable up to 10 minutes post-ablation (Fig. 1D, 1E). *ECM Ablation:* The impact of ablation on ECM SHG signal appears highly dependent on pulse energy (Fig. 1H-I), number of pulses (Fig. 1J-K), and depth within the tissue (Fig. 1L-M). Pulse energies at and below ~400nJ did not yield sustained loss of SHG signal at the ablation site (Fig. 1H), while increasing power to 500nJ or more creates voids in the ECM that can be identified immediately following ablation (Fig. 1I). Similarly, 100 or fewer ablation pulses have no effect (Fig. 1J), while increasing past 200 pulses effectively damages the collagen (Fig. 1K). Finally, depth within the tissue had a profound impact on the efficacy of ablation, with ablation being most successful between 0-30µm below the surface (Fig. 1M), and being ineffective at lower depths (Fig. 1L). High ablation power or pulse number causes collateral tenocyte necrosis via membrane rupture or shockwave-induced disruption, requiring careful optimization of pulse energy, count, and depth to assess effects on cells and ECM.

DISCUSSION: We establish AFL ablation as a precision method to isolate the roles of tendon components in inflammation and healing. Vascular injury[7] and cell necrosis[8] activate inflammation, whereas matrix microdamage alone may not, highlighting the need to decouple these signals. Our results show that AFL ablation enables selective ablation of individual tenocytes, inducing early necrotic changes with increased PI uptake while preserving the surrounding ECM, confirming that cellular injury can be selectively modeled without matrix disruption. ECM ablation proved more challenging: although parameter ranges of pulse energy, pulse number, and tissue depth were identified that effectively reduced SHG signal and generated matrix voids, excessive energy or pulses caused unintended tenocyte necrosis. Thus, while precise cell ablation has been achieved, further optimization is needed to reproducibly damage matrix without collateral cellular injury. Future integration of vascular ablation will complete this triad, enabling mechanistic dissection of how microvascular compromise interacts with cell and matrix injury. By defining the relative contributions of each component to productive versus pathological inflammation, this platform establishes the foundation for precision strategies to restore tendon healing and prevent chronic degeneration.

SIGNIFICANCE/CLINICAL RELEVANCE: By pinpointing how cells, matrix, and (ultimately) vasculature individually drive tendon inflammation and repair, this platform opens the door to precision therapies that transform chronic, ineffective healing into functional recovery.

REFERENCES: [1]Kaux, JF+ *J Sports Sci Med* 2011. [2]Andarawis-Puri, N+ *J Orthop Res* 2018. [3]Jomaa, G+ *BMC Musculoskelet Disord* 2020. [4]Adam, B+ J *Musculoskelet Disord Treat* 2018. [5]Stoychev, V+ *Curr Rev Musculoskelet Med* 2020. [6]Nishimura, N+ *Proc SPIE* 2006. [7]Manon-Jensen, T+ *J Throms Haemost* 2016. [8]Yang, Y+ *Mil Med Res* 2015.
ACKNOWLEDGEMENTS: NIH R01AR084173, NIH R01EB033179, NSF DGE 2139899, Cornell SPROUT.

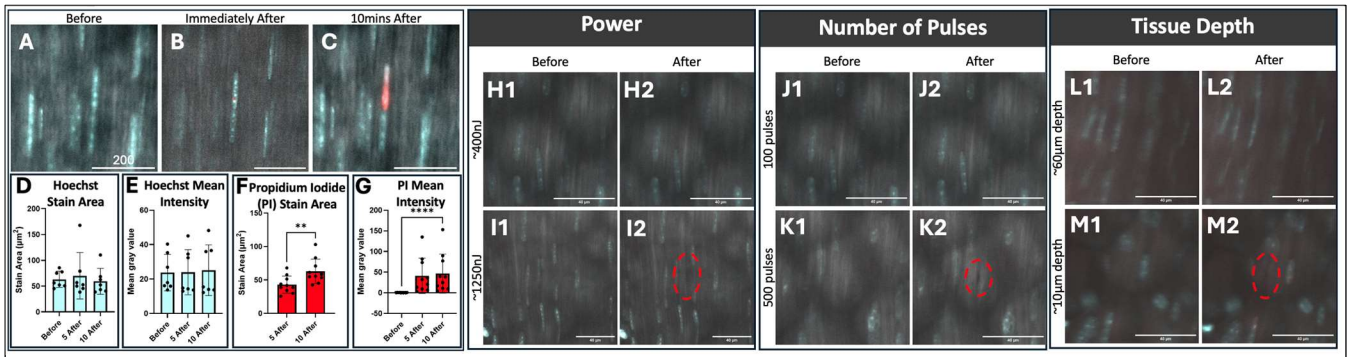

Fig 1: (A–C) Representative tenocyte before ablation, 5 s after, and 10 min after. Live cells are shown in blue; dead cells in red. Quantification of image stacks showed no change in (D) Hoechst area or (E) intensity but increased (F) PI area and (G) mean intensity, confirming membrane damage. (H–M) ECM ablation assessed by SHG signal. No signal loss was observed with low power (H1–H2), low pulse number (J1–J2), or greater depth (L1–L2), indicating intact ECM. In contrast, high power (I1–I2), high pulse number (K1–K2), and shallower depth (M1–M2) caused SHG loss, consistent with ECM damage.